

Interaction of 1-hexyl-3 methylimidazolium bromide ionic liquid with methylparaben drug in aqueous solution: Conductometric and molecular dynamics studies

Roghayeh Darvishi Gilandooz

University of Guilan

bahram ghalami-choobar

b-ghalami@guilan.ac.ir

University of Guilan

mohaddeseh habibzadeh Mashatooki

University of Guilan

Research Article

Keywords: 1-hexyl-3-methylimidazolium bromide, Methylparaben, Fuoss-Onsager, Molecular dynamic simulation, Conductometry

Posted Date: September 2nd, 2024

DOI: <https://doi.org/10.21203/rs.3.rs-4516305/v1>

License:  This work is licensed under a Creative Commons Attribution 4.0 International License.

[Read Full License](#)

Version of Record: A version of this preprint was published at Chemical Papers on February 25th, 2025. See the published version at <https://doi.org/10.1007/s11696-025-03946-4>.

Interaction of 1-hexyl-3 methylimidazolium bromide ionic liquid with methylparaben drug in aqueous solution: Conductometric and molecular dynamics studies

Roghayeh Darvishi Gilandooz, Bahram Ghalami-Choobar*, Mohaddeseh Habibzadeh Mashatooki,

Department of Applied Chemistry, Faculty of Chemistry, University of Guilan, P.O. Box: 19141, Rasht, Iran

* Corresponding Author; Email :B-Ghalami@gilan.ac.ir

Abstract

In this research, the thermodynamic properties and molecular interactions of 1-hexyl-3-methylimidazolium bromide + methylparaben + water system were reported using conductometric method and molecular dynamics simulations. The conductometric data were collected for ionic liquid from 0.0012 to 0.1983 mol.kg⁻¹ on various molality of methylparaben in aqueous solution ($m_{MP} = 0.0000, 0.0005$ and 0.0010 mol.kg⁻¹) at $T = (300.2, 310.2$ and 320.2) K and $P=0.1$ MPa. Fuoss-Onsager equation was applied to get the ion association constants and limiting molar conductivities of ionic liquid and to determine the thermodynamic of ion association. Moreover, molecular dynamics simulations were made to understand the interactions between ionic liquid and methylparaben at the molecular and microscopic level. Radial distribution functions, root mean square deviations, hydrogen bonding and van der Waals and EL interactions were obtained. Furthermore, the diffusion coefficients of ionic liquid in methylparaben and water mixtures were obtained from MD simulation to calculate the molar conductivity of $HMIm]Br$ using Einstein's Nernst equation at $T=310.2$ K and were in agreement with experimental molar conductivity.

Keywords: 1-hexyl-3-methylimidazolium bromide; Methylparaben; Fuoss-Onsager; Molecular dynamic simulation; Conductometry

1 Introduction

Conductivity and solubility are the important physicochemical properties which are needed for drug discovery and development. The low solubility of some drugs slows down their dissolution and absorption in the body [1]. The reliable drug solubility data are required to design the suitable pharmaceutical drug delivery [2-3], formulating of drug with low solubility [4], crystallization [5], considering the absorption, and solubilization mechanism [6-7]. Various molecules used as pharmaceutical causes have very poor solubility in water and biological surroundings, so this significantly limits their therapeutic use. Ionic liquids (ILs) were recently used as a new solvent in pharmaceutical processes. Therefore, the ion association performance of ILs in the existence of a drug is a deep insight. ILs are used to effectively dissolve a range of sparingly soluble compounds by means of their ability to interact with solutes [8]. They present the remarkable features such as high electrical conductivity, nonflammability and satisfactory solvating properties for mixtures [9-13]. ILs are also utilized in multi-disciplinary sciences such as electrochemistry, separation processes, synthesis and especially in drug manufacturing [14]. The ILs and drugs interactions would be a requirement influence evaluates the solubility of drugs. To this aim, there are some information regarding the studies of governing on ILs and drug molecular interactions investigated by electrical conductance [15]. Low water solubility of drug nominees is a main challenge in the pharmaceutical manufacturing where 40% of all recently industrialized drugs are generally low soluble or insoluble in water [16-22]. In recent years, ILs were used to increase the solubility of drugs, which can be mentioned in the following works:

Shekaari et al [22] measured the density and electric conductivity for systems containing acetaminophen and 1-octyl-3-methyl imidazolium bromide in aqueous solution at $T = (293.15-308.15)$ K. The limiting molar conductivities (Λ_0) and ion association constants (K_a) were determined using low concentration Chemical Model (lcCM). Zafarani-Moattar et al [23] investigated the influence of some ILs on the thermodynamic functions of acetaminophen drug using lcCM. Shekaari et al [15] determined the molar conductivities of 1-alkyl-3-methylimidazolium bromide on various concentrations of aspirin in acetonitrile solutions. They analyzed the obtained data using lcCM. The electrical conductivities the sodium salts of alkyleparabens salts were studied by Apelblat et al [24]. Experimental data were interpreted using the Quint–Viallard conductivity equations. Paluch et al determined the solubility of acetaminophen in water [25]. They found it considerable disturbs the obtained solvation free

energy of acetaminophen. Maginn et al [26] obtained the some ILs properties using the experiment and simulation studies. Dasari et al [27] performed the molecular dynamics simulation of the drug, LASSBio-294, in water and seven ionic liquids (ILs): 1-ethyl-3-methylimidazolium methylphosphonate, 1-ethyl-3-methylimidazolium methylphosphonate imidazolium, 1-ethyl-3-methylimidazolium acetate, 1-butyl-3-methylimidazolium acetate, 1,3-Dimethylimidazolium methylphosphonate, 1-ethyl-3-methylimidazolium glycinate, ethylammonium acetate and calculated the atom-atom radial distribution functions (RDFs). Basouli et al [28] made the molecular dynamics simulation of 1-ethyl-3-methylimidazolium methylsulfate [Emim][MeSO₄] at various temperatures and ambient pressure to obtain the relation between counter ions exchange and macroscopic diffusion process.

In this research, in continuation of our previous works [29-30], we investigated the thermodynamic properties of 1-hexyl-3-methylimidazolium bromide ([HMIm]Br) ionic liquid in a solvent mixture of methylparaben (MP) and water at T = (300.2-310.2-320.2) K through experiments and molecular dynamics simulations. Molar conductivity was used to obtain the K_a and Λ_0 values of the studied ionic liquid using the Fuoss-Onsager equation. Also, we used the K_a values to obtain the standard Gibbs free energy (ΔG°), entropy (ΔS°) and enthalpy (ΔH°). The molecular dynamics simulations were carried out to get more details of the interactions between the HMIm]Br and MP. We determined the RDF, root mean square deviation (RMSD), hydrogen bonds (H-Bonds) and van der Waals (vdw) and electrostatic (EL) interactions. Furthermore, we obtained from MD simulation to determine the molar conductivity of HMIm]Br by Einstein's Nernst equation [30] at T=310K.

2 Method

2.1 Conductometric measurements

2.1.1 Materials

1-Bromohexane(>99%), N-methylimidazole (>99%), ethyl acetate and MP were purchased and completely were of analytical reagent grade. Specification of the material used and chemical companies were illustrated in Table 1. The double distilled and deionized water was used to prepare the stock solutions.

2.1.2. Synthesis of ionic liquid

The [HMIIm]Br was manufactured in according to the previous works [29-30] through direct alkylation of N-methylimidazole. 1-Bromohexane and ethyl acetate was introduced drop by drop to the N-methylimidazole solution that was iced in a bath and in a round bottom. Then, the made solution was reflexed under a nitrogen atmosphere for 72h at T=353.2 K. The obtained mixture was moved apart from reagents and then rinsed triply with ethyl acetate to remove the exceed 1-bromohexane. Trace amount of humidity was eliminated by the high vacuum pumping for at least 24 h. The obtained ionic liquid was verified FTIR spectroscopy. Chemical structure and FTIR spectroscopy of [HMIIm]Br were presented in Fig. s1 and Fig.s2 respectively (see supporting information).

2.1.3. Apparatus and procedure

All of conductometric data were get using of a digital conductometer (Proline) with fluctuations of $0.01\mu\text{s.cm}^{-1}$. Before the conductometric measurements, conductometer was calibrated with aqueous KCl solution. At first, the 25 ml of pure solvent was put in the conductometric cell and was closed. Then, the [HMIIm]Br was introduced to the cell containing solvent with a Hamilton syringes (CH-7402 Bonaduz) based on standard addition method. To keep a constant temperature for the test solution, a GFL circulation water bath was utilized at $T = (300.2, 310.2$ and $320.2)$ KK with an accuracy of 0.1 K. The conductivities of [HMIIm]Br solutions were generally corrected to regard the conductivity of pure solvent.

2.2. Computational Details

The NAMD-2.12 package [31] with CHARMM-27 and CHARMM-36 [32] force fields were applied to all simulations. Also, VMD[33] package was used for graphical visualization and analysis. Temperature and pressure was controlled using berendsen thermostat and langevin barostat, respectively [28]. The [HMIIm]Br and MP PDB files were taked from Marvin software [34]. Swiss Param[35] and REDDB[36] web servers were utilized to get the topology and charge data, respectively. The TIP3P[37] model was specified for water molecules and the explicit solvent was considered. The periodic boundary conditions were employed to all commands and the simulation time step was fixed to 1 femtoseconds. The made procedure of simulation for considered systems was including “minimization, annealing, and a final 100 nanosecond isothermal-isobaric (NPT) production simulation”[38-39]. The Berendsen thermostat [40] and Langevin barostat was used to control the temperature and pressure during the NPT production

simulation [41]. Lennard-Jones “12-6” was used to recognize the nonbonding interactions between atoms of [HMIm]Br and MP molecules. interactions were considered with particle mesh Ewald with a cut-off of 10nanometers, and vdw cut-off was used with alike value [1]. At the first step, 3 [HMIm]Br molecules were inserted in a box with dimensions of (70.08Å × 70.07Å × 70.14 Å) to equilibrate the system. During heating step the system’s temperature brought to a 310 K. The final 100 nanosecond MD simulation were done. The next step, was to equilibrate the MP molecules in a box of (70.08Å × 70.13Å × 70.07 Å) for 100 nanosecond. Finally, to observe the aggregation of HMIM-Br and MP molecules and the effect of their presence on each other’s ,a mixed system of these molecules were made in a box dimension of (104.52Å × 101.09Å × 98.12 Å) and a 100 nanosecond MD simulation in NPT ensemble (see Fig. s3 in supporting information).

3. Results and discussion

3.1. Conductometric study

3.1.1 Determination of molar conductivity and calibration

Conductometric data were made for the binary [HMIm]Br + water system. The molar conductivity (Λ) values were determined by using conductometric data. In table2, the Λ values were illustrated as a function of the molal concentration of the ionic liquid (m_{IL}) at $T = (300.2, 310.2$ and 320.2) K. Fig. 1 shows the found data are in good agreement with literature at $T = (308.2$ and 310.2) K temperatures [43].

3.1.2 Determination of limiting molar conductivity

The Λ values of HMIm]Br solutions as function of MP molal concentration ($m_{MP}=0.000, 0.005$ and $0.010 \text{ mol.kg}^{-1}$) in aqueous system were given in Table 2 at temperature of 300.2, 310.2 and 320.2 K. Moreover, Figs. 2-4 show that the Λ values of HMIm]Br decreases with growing the concentration of [HMIm]Br while it increases with growing the temperature at the similar concentration of MP. The comparable trends have been stated for ILs in the literatures [22,23,29,30,43,45]. It can be explained that the Λ values of HMIm]Br decreases with increasing the concentration of [HMIm]Br as a result of the growth in the ion pair formation[30]. In addition, the ion association and relaxation effect between anion and cation of HMIm]Br

enlarges with a growth in its concentration and consequently the mobility of the charge transporters moderates. The effect of these factors leads to the decrease of Λ values in the concentrated area. Moreover, Figs. 2-4 indicate that the Λ value increases with the increase in temperature. This effect can be mentioned to the mobility increased of free ions with temperature raising. Fig. 5 shows that the Λ value of [HMIIm]Br decreases with the increase in MP concentration at $T= 300.2$ K. The result of MP concentration on the [HMIIm]Br Λ values is a consequence of the valuable ions solvation by MP and subsequently the increase in solvent viscosity. However, electrical conductivity decreases with increasing the solvent viscosity [29].

3.1.3 Correlation of molar conductivity with Fuoss-Onsager equation

Fuoss_Onsager model was used to correlate the Λ values in according to the following equation:[29]

$$\Lambda = \Lambda_0 - SC^{\frac{1}{2}}\alpha^{\frac{1}{2}} + EC\alpha \log C\alpha + JC\alpha - K_A C\alpha \gamma^2 \Lambda \quad (1)$$

$$J = \sigma_1 \Lambda_0 + \sigma_2 \quad (2)$$

$$S = \alpha \Lambda_0 + \beta_0 \quad (3)$$

$$\alpha = \frac{0.8204 \times 10^6}{(\varepsilon T)^{\frac{3}{2}}} \quad (4)$$

$$\beta = \frac{82.50}{\eta(\varepsilon T)^{\frac{1}{2}}} \quad (5)$$

$$E' = E'_1 \Lambda_0 + E'_2 \quad (6)$$

$$E'_1 = \frac{2.942 \times 10^{12}}{(\varepsilon T)^3} \quad (7)$$

$$E'_2 = \frac{0.4333 \times 10^8}{\eta(\varepsilon T)^2} \quad (8)$$

In above equations, C is the molar concentration (mol.L^{-1}) and γ is dissociation degree. The S and E constants can be calculated using dielectric constant (ε), kelvin temperature (T) and the viscosity (η). J term, σ_1 and σ_2 indicate the ions -solvent interactions and are distance functions [29,44]. The obtained values of K_A , Λ_0 , and R for [HMIm]Br on $m_{\text{MP}} = 0.00, 0.005$ and $0.010 \text{ mol.kg}^{-1}$ on various temperatures were illustrated in table 3. These results indicate that K_A and Λ_0 values increase with the increase in temperature and MP concentration. In addition, the ΔG° values decreases with the increase in temperature and MP concentration. It can be describe that the interactions of the ions of HMIm]Br and MP with increasing MP concentration become stronger [45]. The obtained values of distance parameters (R) decrease as the MP concentrations solutions increase. The small values of (R) for [HMIm]Br is indicated to the strong ionic association.

3.1.2. Thermodynamics of ion association

The thermodynamic properties were determined using the ion aggregation constant with the help of the following equations:

$$\Delta G^\circ = -RT \ln K_A \quad (9)$$

$$\Delta S^\circ = \frac{\Delta H^\circ - \Delta G^\circ}{T} \quad (10)$$

$$\frac{d(\frac{\Delta G}{T})}{dT} = -\frac{\Delta H}{T^2} \quad (11)$$

The values of ΔG° , ΔH° and ΔS° were given in **Table 3**. The results obtained from **Table 3** show that formation of ion pair is spontaneous phenomenon and this process growths with increasing temperature. Here in, this phenomenon has caused the positive entropy in the range of temperature. Due to the unbinding of solvent molecules from solvation layers as association takes place and increasing the freedom degrees number may be attributed the positive values of ΔS° to this process. The positive values ΔH° show that the process of ion pair formation is endothermic. It can be expected that the ordinary attractions of anions and cations via coulomb forces, vdw forces and H- bonds, may not be adequate to help the ion pair formation.

3.2 Simulation

3.2.1 Calculation of molar Conductivity

The molar conductivity can be calculated using a direct connection between diffusion coefficients of cations and anions via the Nernst–Einstein (NE) equation [46]:

$$\Lambda_{NE} = \frac{N_A e^2}{k_B T} (z_+^2 D_+ + z_-^2 D_-) \quad (12)$$

where Λ_{NE} is the NE molar conductivity, D is the self-diffusion coefficient of ions, and other symbols have usual meaning. [47]. In these calculations, $z_+ = z_- = 1$ was used for [HMIm]Br ionic liquid. The transport of anion and cation were determined by calculation the mean square displacement (MSD) from MD simulation. The Einstein relation was used to calculate the D values in according to the equation 13[48] :

$$(13) D = \frac{1}{6} \lim_{t \rightarrow \infty} \frac{d}{dt} \langle [r_i(t) - r_i(0)]^2 \rangle$$

where the $r_i(t)$ and $r_i(0)$ are the position vectors of the mass center of ion i at time t and 0, respectively. The self-diffusion coefficient of cations and anions was computed based on the MSD calculations using the “diffusion coefficient master” of VMD software. The self-diffusion coefficient results were illustrated in table s1. The calculated theoretical and experimental measurements of molar conductivity values of the ionic liquid in the presence and absence of MP drug were calculated using the diffusion coefficient and tabulated in Table 4. In according to the values illustrated in the table 4, the experimental data is in good agreement with the simulation results. Therefore, the simulation results can be used to describe the molecular aggregation between the MP drug and [HMIm]Br at the atomic-level interactions.

3.2.2 RMSD

The RMSD of the [HMIm]Br ionic liquid in the presence and absence of MP drug was calculated to show the stability of ionic liquid and drug during the aggregation process. The equation (14) was used to compute the RMSD of ionic liquid and drug [49]:

$$\text{RMSD} = \sqrt{\frac{1}{N} \sum_{i=1}^N (r_i(t + \Delta t) - r_i(t))^2} \quad (14)$$

Where N is the numbers of atoms and other symbols have usual meaning. Figs. 6 and 7 display the RMSD (Å) variation of ionic liquid atoms in absence and attendance MP drug on aqueous solution, respectively. It can be seen that the configuration of ionic liquid was not changed after relaxation. The RMSD values were demonstrated in table 5. It can be seen, the RMSD (Å) values of ionic liquid in the attendance of MP drug are more than the correspond values in the absence of MP drug. It can be described in terms of the strong interactions between [HMIM]Br and MP drug.

3.2.3. *RDF*

In a system contain particles, the local densities of the particle i all over the place j along the radial direction can be described through RDF [50]. To analyze the HMIMBr-water and HMIMBr-MP-water interactions, the radial distribution functions of these pairs were calculated the 100 ns of time simulation paths (Fig. 8a-d). The comparison of intensity and position of the first peak in Fig.8c-d the indicate that aggregations of HMIMBr ionic liquid increases in the presence of MP drug. The found results are in agreement with experimental data which K_A values raise with the increase in MP concentration.

3.2.4. *H-Bonds*

The average number of HMIMBr –water and HMIMBr -MP-water molecules H-Bonds was computed in the studied systems by using VMD software all through the last 10 ns of the simulation paths. Fig. 9a-d shows that distribution of H-Bonds in all cases has a normalized distribution. Also, Table 6 gives the obtained results of H-Bonds for studied systems. Fig.10 shows, the average number of normalized H-Bond for HMIMBr and MP drug in mixture are shown an increase compared to alone HMIMBr and MP drug in aqueous system. On the other hand, the strong hydrogen bond happens between HMIMBr ionic liquid and MP drug molecules.

3.2.5. *Interaction energies*

Interaction energies of the system were computed by “NAMD Energy” of VMD software. The normalized distribution of EL interactions and vdW energies was utilized to assess the forces

between atoms and molecules (see Fig.11 a-d and Fig.s4 in supporting information). The average value of the interaction energies was considered by fitting the distribution function with population data. Fig.12 shows the relationship of EL interactions and vdW energies between MP molecules and HMIMBr ionic liquid in the absence and presence of MP drug. Moreover, the found data were demonstrated in table 7. That observes, the EL interactions contribution between MP drug and ionic liquid are more than the vdw forces in addition to H- bonds. Furthermore, the contribution of EL interactions between HMIMBr ionic liquid in water + MP are more than the EL interactions HMIMBr ionic liquid but the contribution of EL interactions between MP molecules in water + ionic liquid are less than the EL interactions MP molecules in aqueous solution. However, the obtained results show that the ordinary attractions of anions and cations via coulomb forces, vdw forces and H-Bonds are not adequate to help the ion pair formation. Therefore, the EL and H-Bonds interactions play insignificant role on ion pair formation in MP + HMIMBr ionic liquid system. On the other hand, ion pair formation cannot be enthalpy driven.

4. Conclusions

The interactions of HMIMBr ionic liquid with MP drug in water as solvent were investigated by experimental and theoretical studies. The influence of temperature and MP concentration on the interaction of HMIMBr ionic liquid with MP were studied. The K_a and Λ_0 values of ionic liquid were achieved using Fuoss-Onsager equation and applied to get the standard Gibbs free energy, enthalpy, and entropy variations. MD simulations were made to know the aggregations at the atomic-level interactions. The calculated molar conductivity of HMIMBr ionic liquid were made in the presence and absence of MP drug and found the good agreement between the experimental and simulation results. Also, The RDF results showed that the tendency for aggregation increases in the presence

of MP which is in agreement with changes of KA values. It can be concluded that HMIMBr ion-pair association in water+MP mixtures is endothermic and entropy driven.

Acknowledgement

This work has been supported by University of Guilan.

Declarations

Ethical Approval

This declaration is “not applicable”.

Competing interests

The authors declare that they have no known competing financial interests.

Funding

This work has been supported by University of Guilan , However, there is no fund number

Availability of data and materials

The calculated data can be accessed

References

- [1] Mirheydari ,S. N .Barzegar-Jalali ,M. Shekaari ,H. .Martinez,F..Jouyban ,A.(2019). Experimental determination and correlation of lamotrigine solubility in aqueous mixtures of 1-octyl3-methyl imidazolium bromide ionic liquid at various temperatures, *The Journal of Chemical Thermodynamics* 135: 75–85. DOI:10.1016/j.jct.2019.03.024.
- [2] Shayanfar, A. Soltani, S. Jabbarifar, F. Tamizi, E .W, E. Jr, A. Jouyban, A. (2008). Solubility of anthracene in ternary solvent mixtures of 2, 2, 4-trimethylpentane + 2-propanone + alcohols at 298.2 K, *Journal of Chemical & Engineering Data*.53:890–893.DOI:10.1021/je8000415.

[3] Delgado, D.R. Almanza, O.A. Martínez, F. Peña, M.A. Jouyban, A. E, W. Jr ,A.(2016). Solution thermodynamics and preferential solvation of sulfamethazine in (methanol + water) mixtures, *The Journal of Chemical Thermodynamics*.97 :264–276.

[4] van der Vossen, A.C. van der Velde, I. Smeets, O.S.N.M. Postma, D.J. Eckhardt, M. Vermes, A. Koch, B.C.P. Vulto, A.G. Hanff , L.M. (2017). Formulating a poorly water soluble drug into an oral solution suitable for paediatric patients; lorazepam as a model drug, *European Journal of Pharmaceutical Sciences*. 100 : 205–210. DOI:10.1016/j.ejps.2017.01.025.

[5] Sriamornsak, P. Burapapadth, K.(2015).Characterization of recrystallized itraconazole prepared by cooling and anti-solvent crystallization, *Asian Journal of Pharmaceutical Sciences*.10:230–238. <https://doi.org/10.1016/j.ajps.2015.01.003>.

[6] Jouyban, A.(2010)..Handbook of Solubility Data for Pharmaceuticals, *CRC Press, Taylor & Francis*. DOI:10.1201/9781439804889.

[7] Faller, B. Ertl ,P.(2007). Computational approaches to determine drug solubility, *Advanced Drug Delivery Reviews* .59 :533–545.DOI:10.1016/j.addr.2007.05.005.

[8] Curreri, A.M. Mitragotri, S.and Tanner, E. E. L.(2021). Recent Advances in Ionic Liquids in Biomedicine, *Advanced Science* .8 : 2004819. DOI:10.1002/advs.202004819.

[9] Watanabe, M..Tokuda, H ..Tsuzuki, S. Susan, M. A. B. H. Hayamizu ,K.(2006). How ionic are roomtemperature ionic liquids? An indicator of the physicochemical properties. *Journal of Physical Chemistry B* .110:19593-19600. DOI:10.1021/jp064159v.

[10] Chaban, V. V.. Voroshlyova, J. V Kalugin. O. N. (2011) . A new force field model for the simulation of transport properties of imidazolium-based ionic liquids. *Physical Chemistry Chemical Physics*..466 :7910-7920. DOI:10.1039/C0CP02778B.

[11] Duan, E. H. Guo, B. Zhang, M. M..Ren, A. L.Yang, B. B. Zhao, D. S.(2010).Electrical conductivity of caprolactam tetrabutylammonium bromide ionic liquids in aqueous and alcohol binary systems. *Journal of Chemical & Engineering Data*.55 : 4340-4342. <https://doi.org/10.1021/je100085r>.

[12] Ohno ,H. Ogihara, W. Sun , J. Forsyth , M..MacFarlane , D. R. Yoshizawa , M.(2004). Ionic conductivity of polymer gels deriving from alkali metal ionic liquids and negatively charged polyelectrolytes. *Electrochimica Acta*..49:1797-1801. DOI:10.1016/j.electacta.2003.12.011.

[13] Noda, A. Hayamizu, K. Masayoshi ,W.(2001).Pulsed-Gradient Spin–Echo ^1H and ^{19}F NMR Ionic Diffusion Coefficient, Viscosity, and Ionic Conductivity of Non-Chloroaluminate Room-Temperature Ionic Liquids . *Journal of Physical Chemistry B* .105 : 4603-4610. DOI:10.1021/jp004132q.

[14] Kim, H. Shim,J.Y..(2009). Solvation of carbon nanotubes in a room-temperature ionic liquid. *ACS Nano*, 3:1693-1702. DOI:10.1021/nn900195b.

[15] Shekaari, H. Zafarani-Moattar , M.T. and Mirheydari , S.N.(2016).Conductometric Analysis of some Ionic Liquids, 1-Alkyl-3-methylimidazolium Bromide with Aspirin in Acetonitrile Solutions. *Physical Chemistry Research* .4 : 355-368. DOI:10.22036/pcr.2016.14658.

[16] Kouki ,N. Tayeb, R. Dhahbi ,M.(2014). Recovery of acetaminophen from aqueous solutions using a supported liquid membrane based on a quaternary ammonium salt as ionophore. *Chemical Papers*.68:457–464. DOI:10.2478/s11696-013-0479-5.

[17] Kianipour, S. Asghari, A. (2013). Roomtemperature ionic liquid/multiwalled carbon nanotube/chitosanmodified glassy carbon electrode as a sensor for simultaneous determination of ascorbic acid, uric acid, acetaminophen, and mefenamic acid. *IEEE Sensors Journal* .13 :2690-2698. DOI:10.1109/JSEN.2013.2259588.

[18] Suresh Babu , R. Prabhu , P. Anuja, S. (2012). S.Sriman Narayanan, , Electrocatalytic oxidation of acetaminophen using 1-ethyl-3-methylimidazolium tetrafluoroborate-nickel hexacyanoferrate nanoparticles gel modified electrode. *Journal of Chemical and Pharmaceutical Research*.4:3592-3600.

[19] Tavana , T. Khalilzadeh , M.A. Karimi-Maleh , H. Ensafi , A. A..Beitollahi , H. Zareyee, D. (2012). Sensitive voltammetric determination of epinephrine in the presence of acetaminophen at a novel ionic liquid modified carbon nanotubes paste electrode. *Journal of Molecular Liquids*. 168:69-74. DOI:10.1016/j.molliq.2012.01.009.

[20] Chou , F. M. Wang , W. T. Wei , G. T. (2009). Using subcritical/supercritical fluid chromatography to separate acidic, basic, and neutral compounds over an ionic liquid-functionalized stationary phase. *Journal of Chromatography A*.1216: 3594-3599. DOI:10.1016/j.chroma.2009.02.057.

[21] Mizuuchi , H. Jaitely , V. Murdan , S. Florence , A. T. (2008). Room temperature ionic liquids and their mixtures: potential pharmaceutical solvents. *European Journal of Pharmaceutical Sciences* .33: 326-331. DOI:10.1016/j.ejps.2008.01.002.

[22] Shekaari, H. Zafarani-Moattar , M.T. and Ghaffari , F.(2016). Volumetric, Acoustic and Conductometric Studies of Acetaminophen in Aqueous Ionic Liquid, 1-Octyl-3-methylimidazolium Bromide at T = 293.15-308.15 K. *Physical Chemistry Research*.4 :119-141. DOI:10.22036/pcr.2016.12593.

[23] Zafarani-Moattar , M.T . Shekaari , H.and Ghaffari , F.(2017). Effect of Some Imidazolium-Based Ionic Liquids with Different Anions on the Thermodynamic Properties of Acetaminophen in Aqueous Media at T = 293.15 to 308.15 K. *Journal of Chemical & Engineering Data*.62 : 4093–4107. DOI:10.1021/acs.jced.7b00464.

[24] Kroflič, A. Apelblat, A. and Bešter-Rogač, M.. (2012). Dissociation Constants of Parabens and Limiting Conductances of Their Ions in Water. *Journal of Physical Chemistry B* .116:1385–1392. DOI:10.1021/jp211150p.

[25] Paluch, A.s. C.Lourenço, T. Han, F.and Costa, L.T.(2016). Understanding the Solubility of Acetaminophen in 1-n-Alkyl-3- Methylimidazolium Based Ionic Liquids Using Molecular Simulation. *Journal of Physical Chemistry B* .120 :3360–3369. DOI:10.1021/acs.jpcb.5b11648.

[26] Liu, H. Maginn, E. Visser, A. E.. Bridges, N. J and. FoxE. , B (2012). Thermal and Transport Properties of Six Ionic Liquids: An Experimental and Molecular Dynamics Study. *Industrial & Engineering Chemistry Research*.51 : 7242–7254. <https://doi.org/10.1021/ie300222a>.

[27] Dasari, S. , Mallik B. S.(2020).Solubility and solvation free energy of a cardiovascular drug, LASSBio-294, in ionic liquids: A computational study. *Journal of Molecular Liquids* .301: 112449. DOI:10.1016/j.molliq.2020.112449.

[28] Basouli, H. Mozaffari , F. Eslami ,H .(2021).Atomistic insights into structure, ion-pairing and ionic conductivity of 1-ethyl-3-methylimidazolium methylsulfate [Emim][MeSO₄] ionic liquid from molecular dynamics simulation, . *Journal of Molecular Liquids*.331 :115803. DOI:10.1016/j.molliq.2021.115803.

[29] Ghalami-Choobar,B.NosratiFallahkar,T.2019.Thermophysical properties of 1-ethyl-3-methylimidazolium bromide ionic liquid in water + ethylene carbonate mixtures at T =(298.2, 308.2 and 318.2) K. *Fluid Phase Equilibria*. 496: 42-60. DOI:10.1016/j.fluid.2019.05.015.

[30] Ghalami-Choobar,B. Meftah Niaki ,M .(2020). Transport and optical properties of 1-octyl 3-methylimidazolium bromide ionic liquid in water + Ethanol/1-propanol mixtures at T=(298.2, 308.2 and 318.2) K. *Journal of Molecular Liquids* .303: 112534. DOI:10.1016/j.molliq.2020.112534.

[31] Liu H. Maginn ,E.(2012).An MD Study of the Applicability of the Walden Rule and the Nernst–Einstein Model for Ionic Liquids, *Chem Phys Chem*.13: 1701-1707. DOI:10.1002/cphc.201200016.

[32] Phillips,J.C . Braun, R. Wang, W. Gumbart , J. Tajkhorshid, E..Villa, E..Chipot, C .(2005). R.D Skeel; L Kalé; K. Schulten,; Scalable molecular dynamics with NAMD, *Journal of Computational Chemistry* .26 : 1781–1802. DOI:10.1002/jcc.20289.

[33]. Vanommeslaeghe ,K. Hatcher, E. Acharya ,C. Kundu ,S. Zhong, S. Shim,, J. Darian ,E. Mackerell,A.D .(2010).CHARMM general force field: A force field for drug-like molecules compatible with the CHARMM all-atom additive biological force fields, *Journal of Computational Chemistry*.31:671-690. DOI:10.1002/jcc.21367.

[34] Humphrey ,W. Dalke.K, Schulten, A.(1996). VMD: Visual molecular dynamics, *Journal of Molecular Graphics*. 14: 33–38. DOI:10.1016/0263-7855(96)00018-5.

[35] MarvinSketch.(2014).(version 6.2.2, calculation module developed by ChemAxon, <http://www.chemaxon.com/products/marvin/marvinsketch/>).

[36] Zoete,V. Cuendet, A.M. Grosdidier, A. Michelin, O. (2011).SwissParam, a Fast Force Field Generation Tool For Small Organic Molecules. *Journal of Computational Chemistry*. 32 : 2359-68. DOI:10.1002/jcc.21816.

[37] Dupradeau; F.Y .Pigache,A ..Zaffran ,T.Savineau ,C. Lelong, R..Grivel ,N. Lelong ,D.Rosanski, W P. Cieplak.2010. The R.E.D. Tools: Advances in RESP and ESP charge derivation and force field library building, *Physical Chemistry Chemical Physics* .12: 7821-7839. DOI:10.1039/C0CP00111B.

[38]Mark, P. Nilsson, L.(2001).Structure and dynamics of the TIP3P, SPC, and SPC/E water models at 298 K. *Journal of Physical Chemistry A*. 105: 9954–9960. DOI:10.1021/jp003020w.

[39]Habibzadeh Mashatooki, M. Jahanbin Sardroodi, J.(2020).A Molecular Dynamics Study Proposing the Existence of Structural Interaction Between Cancer Cell Receptor and RNA Aptamer . *Journal of Inorganic and Organometallic Polymers and Materials*.30:4520–4532. DOI:10.1007/s10904-020-01740-1.

[40]Habibzadeh Mashatooki , M. Abbasi, A. Jahanbin Sardroodi, J. (2020).In silico studies of the interaction between colon cancer receptor and RNA aptamer in complex with (1 0 1) facet of TiO₂ nanosheet: A molecular dynamics study. *Adsorption*. 26: 941–954. DOI:10.1007/s10450-019-00126-1.

[41] Kubo , R. Toda , M. Hashitsume , N. (1991). Statistical Physics II: Nonequi- librium Statistical

Mechanics, Springer: New York, 2nd ed.

[42]Feller; S.E. Zhang ,Y . Pastor , R. W. Brooks , B.R.(1995).Constant pressure molecular dynamics simulation: The Langevin piston method, *Journal of Chemical Physics*.103:4613–4621 DOI:10.1063/1.470648.

[43] Wang , H. Zuo,Z. Lu, L. Laaksonen ,A. Wang, Y .Lu , X. Ji ,X.(2023).Experimental and theoretical study on ion association in [Hmim] [halide] + water/isopropanol mixtures *Fluid Phase Equilibria*. .566: 113680. DOI:10.1016/j.fluid.2022.113680.

[44] Banjare, M.K. Behera, K. Kurrey, R. Banjare, R.K. Satnami, M.L. Pandey, S. Ghosh, K.K. (2018). Self-aggregation of bio-surfactants within ionic liquid 1-ethyl-3-methylimidazolium bromide: a comparative study and potential application in antidepressants drug aggregation, *Spectrochimica Acta Part A: Molecular and Biomolecular Spectroscopy*.199 :376-386.DOI:10.1016/j.saa.2018.03.079.

[45] Shekaari , H. Kazempour ,A.(2012). Thermodynamic properties of d-glucose in aqueous 1-hexyl-3-methylimidazolium bromide solutions at 298.15K.*Fluid Phase Equilibria*.336 :122–127. DOI:10.1016/j.fluid.2012.08.024.

[46] Afandak, A. Eslami, H. (2017).Ion-Pairing and Electrical Conductivity in the Ionic Liquid 1-n-Butyl-3- Methylimidazolium Methylsulfate [BMIm][MeSO₄]: A Molecular Dynamics Simulation Study. *Journal of Physical Chemistry B* .121:7699–7708.DOI:10.1021/acs.jpcb.7b06039.

[47] Chen, M. Pendrill, R. Widmalm, G. Brady, J. W. Wohlert, J.(2014)..Molecular Dynamics Simulations of the Ionic Liquid 1 n Butyl-3- Methylimidazolium Chloride and Its Binary Mixtures with Ethanol. *Journal of Chemical Theory and Computation*.. 10: 4465–4479. DOI:10.1021/ct500271z.

[48] Onwudiwe, K. Najera, J .Holen, L. Burchett, A.A. Rodriguez, D. Zarodniuk, M . Siri, S and Datta, M.(2024). Dynamical Properties of a Hydrated Lipid Bilayerfrom a Multinanosecond Molecular Dynamics Simulation. *Biophysical Journal*. 123:1098–1105. DOI:10.1016/j.bpj.2024.03.034.

[49] Vanommeslaeghe, K. Hatcher, E. Acharya, C. Kundu, S. Zhong, S. Shim, J. Darian, E. Guvench, O. Lopes, P. Vorobyov, I. Mackerell Jr ,A. D.(2010).CHARMM general force field: A force field for drug-like molecules compatible with the CHARMM all-atom additive biological force fields. *Journal of Computational Chemistry*. 31 :671-690. DOI:10.1002/jcc.21367.

[50] Habibzadeh Mashatooki, M. Ghalami – Choobar ,B.(2021).Characterization of self-aggregated mitomycin C onto the boron-nitride nanotube as a drug delivery carrier: A molecular dynamics investigation. . *Journal of Molecular Liquids*.334:116065. DOI:10.1016/j.saa.2018.03.079.

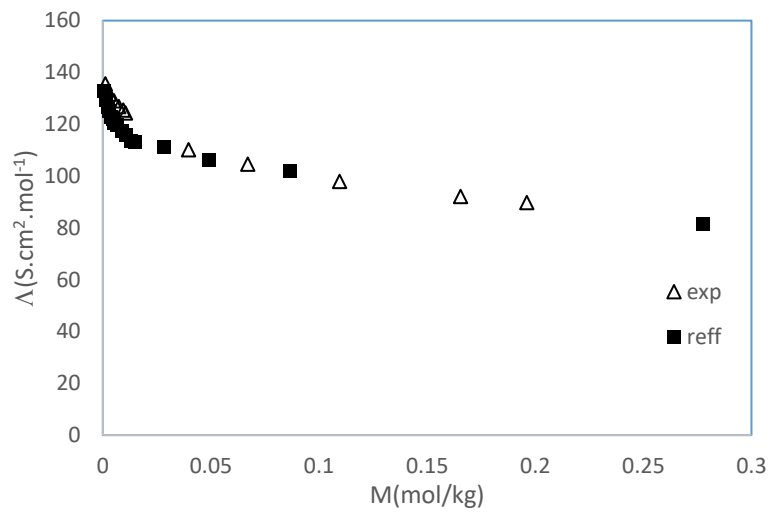


Fig. 1. Comparison of experimental molar conductivities of IL solutions with the literature data [43] Symbols: [Hmim]Br+water: Δ , this work (310.2 K.), \blacksquare , Hui Wang et al (308.2)

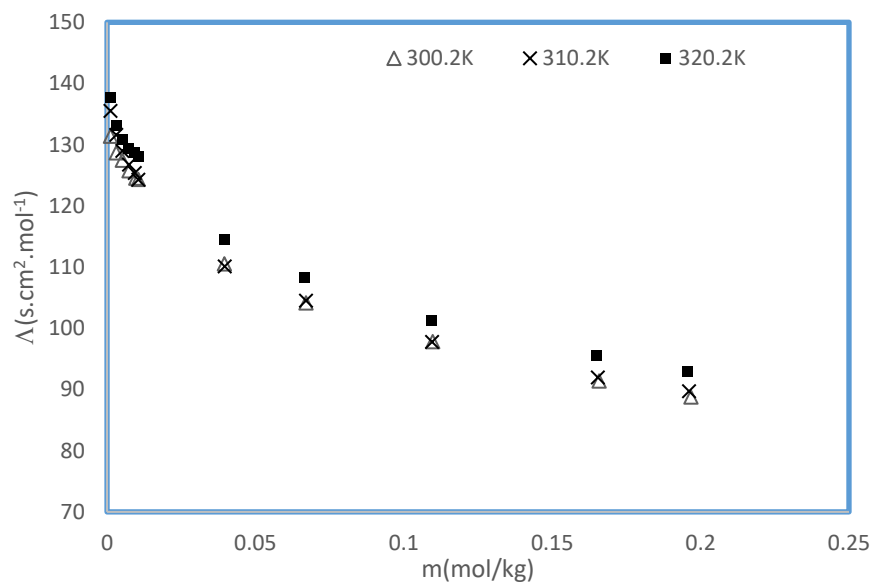


Figure 2. Molar conductivities of [HMIIm]Br as IL molality function on MP 0

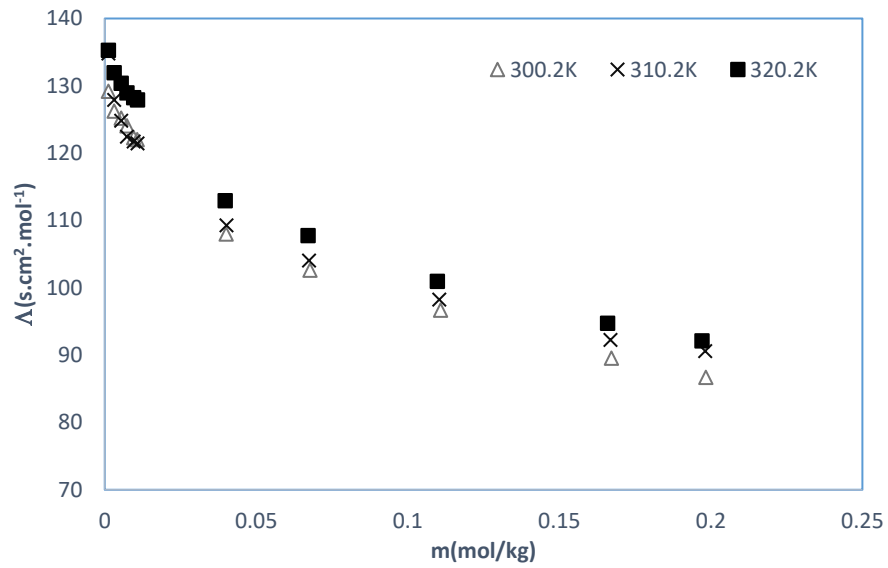


Figure 3. Molar conductivities of [HMIm]Br as IL molality function on MP = 0.005

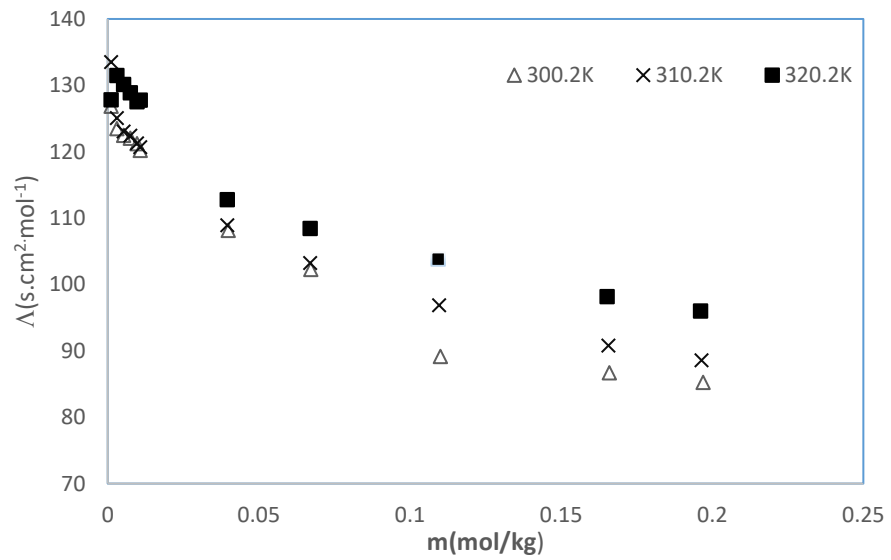


Figure4. Molar conductivities of [HMIIm]Br as IL molality function on MP of 0.01

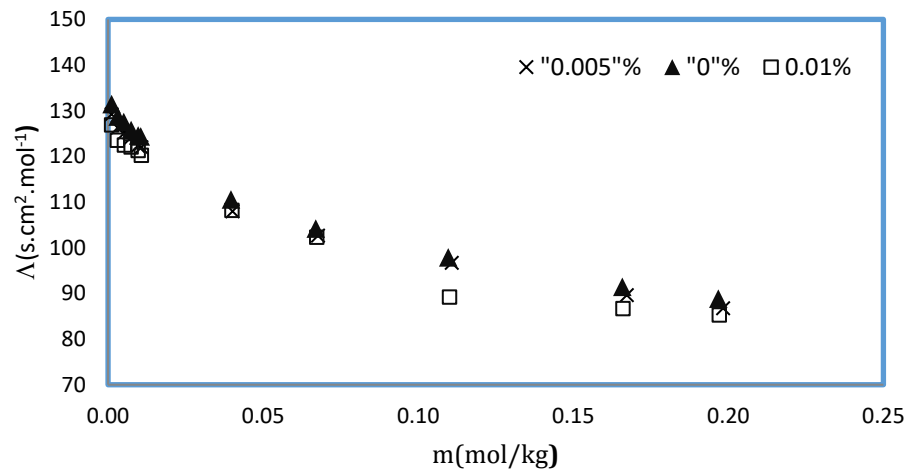


Figure5. Molar conductivities of [HMIIm]Br in MP+ water at T=300.2K

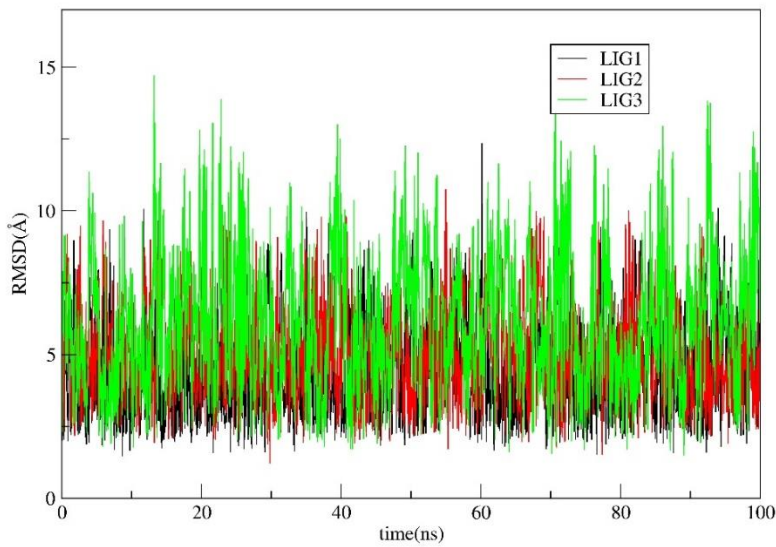


Fig. 6 Representative plots of RMSD of [HMIm]Br in absence of MP

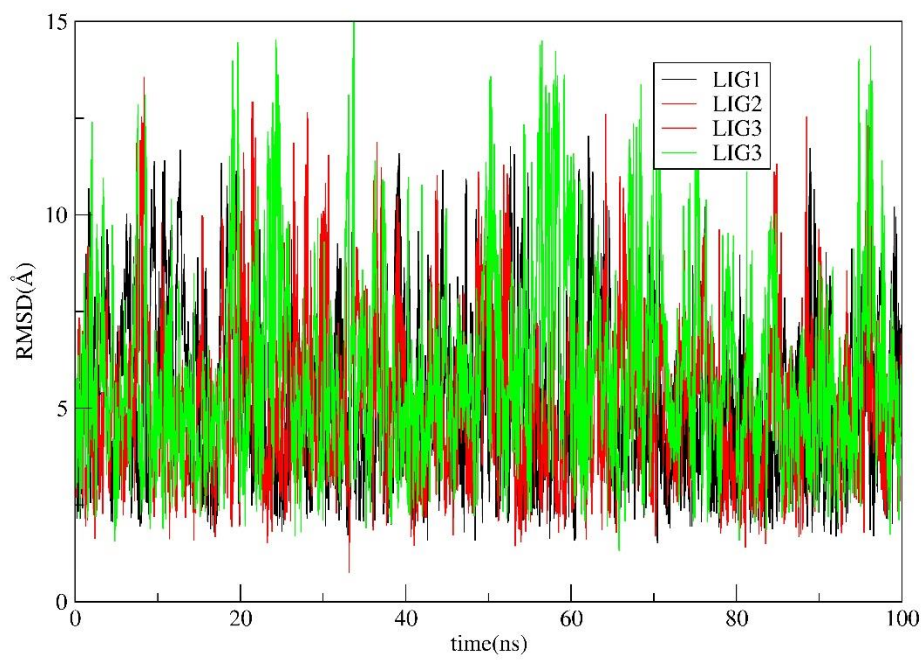
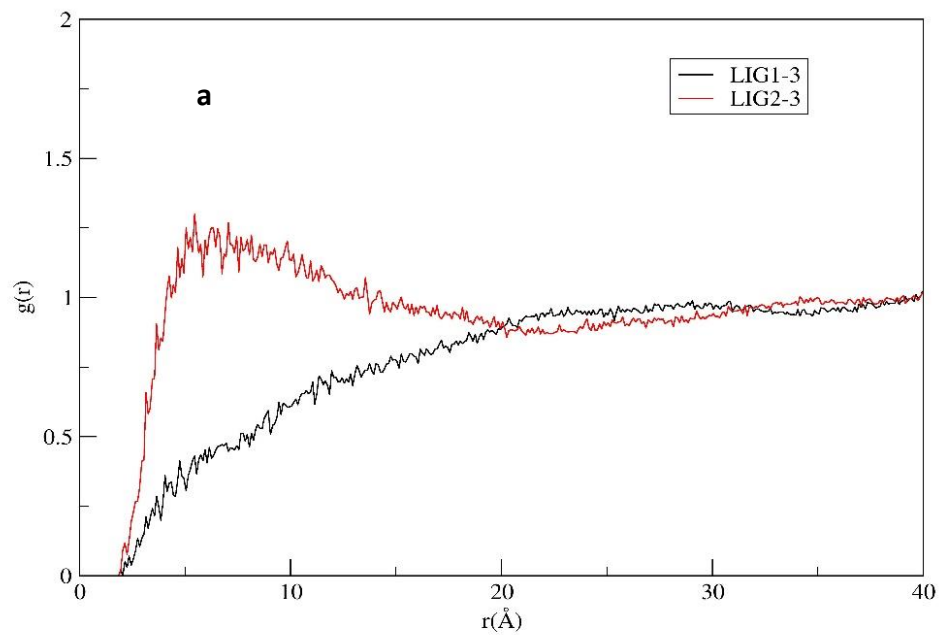
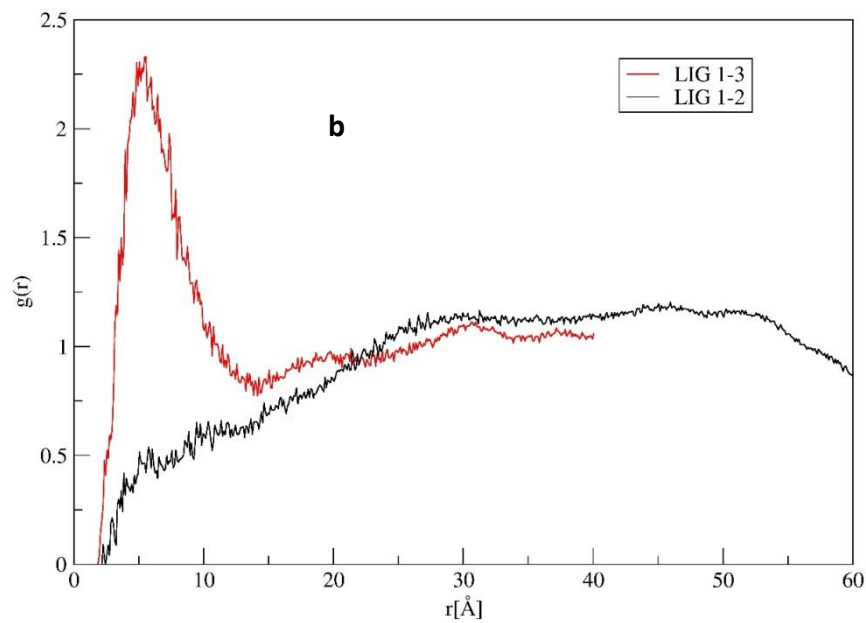


Fig. 7 Representative plots of RMSD of [HMIm]Br in presence of MP





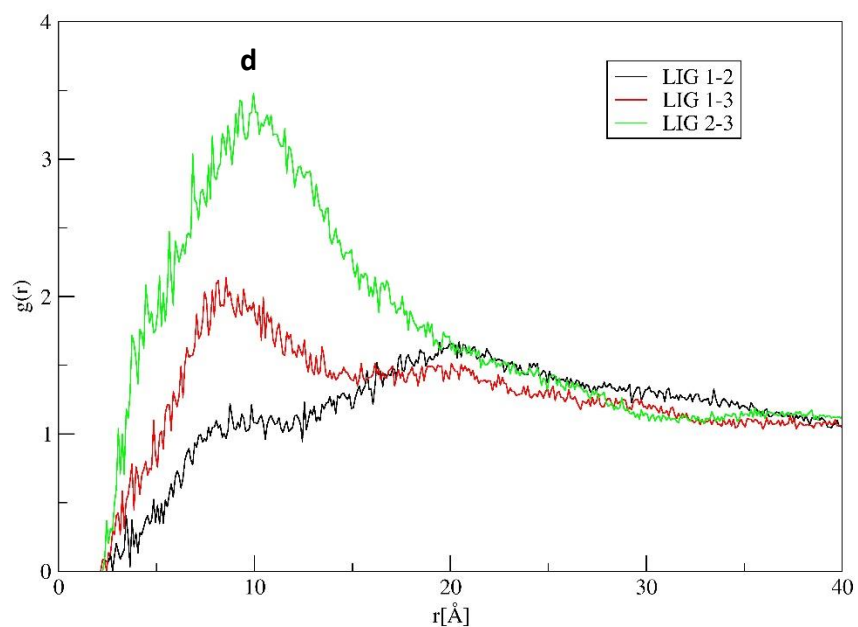
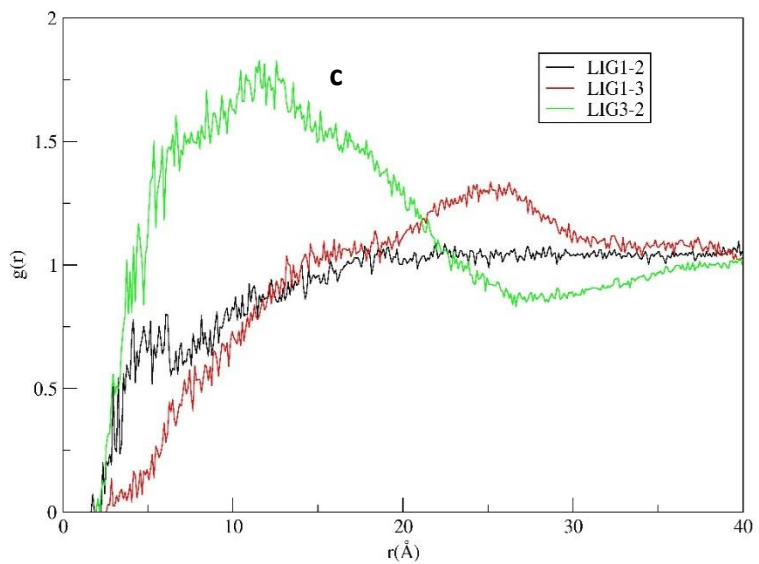
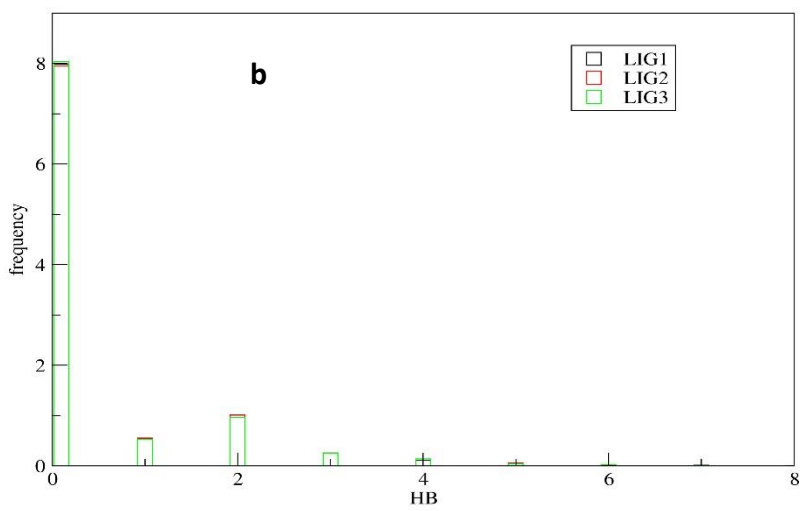
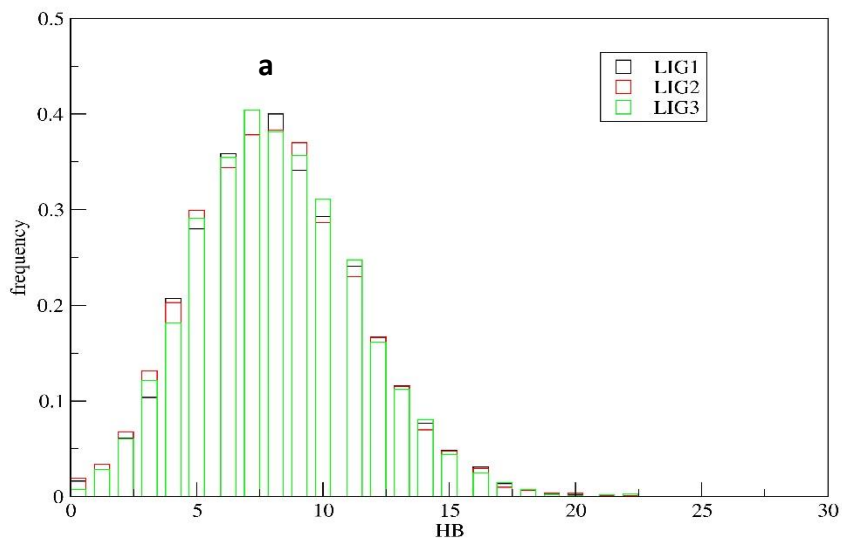


Fig.8 . The RDF plot of MP- MP in water (a) MP- MP in $[HMIm]Br$ + water (b) $[HMIm]Br$ - $[HMIm]Br$ in water (c) $[HMIm]Br$ - $[HMIm]Br$ in MP+water (d)during the last 10 ns of the 100 ns simulation time.



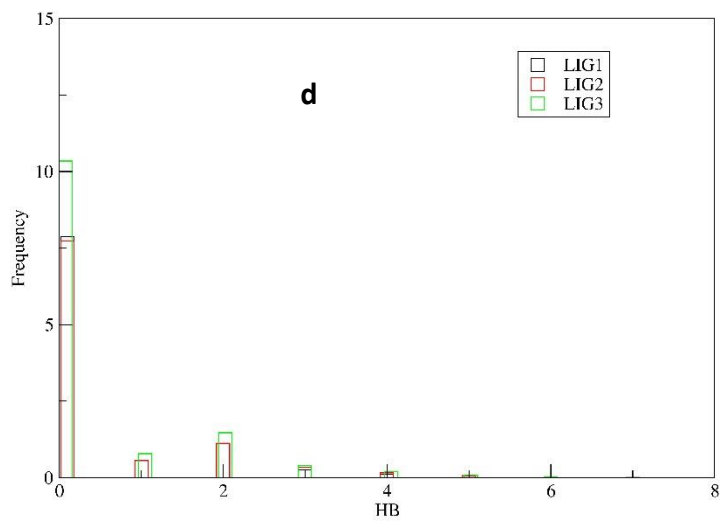
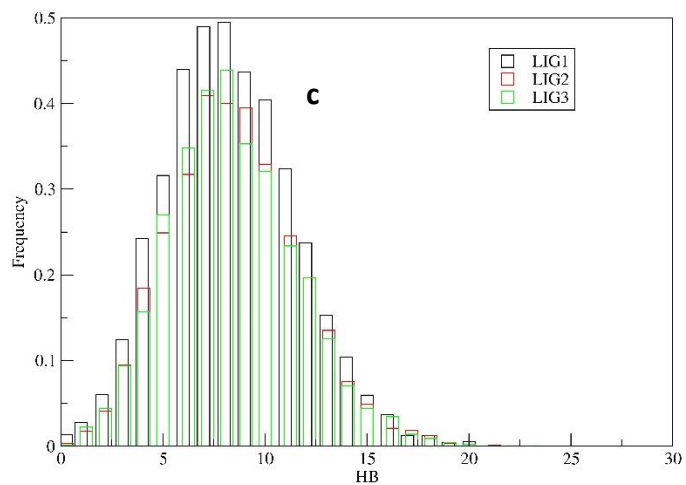


Fig. 9. Normalized distribution of HB of MP in water(a) [HMIIm]Br in water, (b) MP in HMIIm]Br +water(c), and MP in HMIIm]Br +water(d)

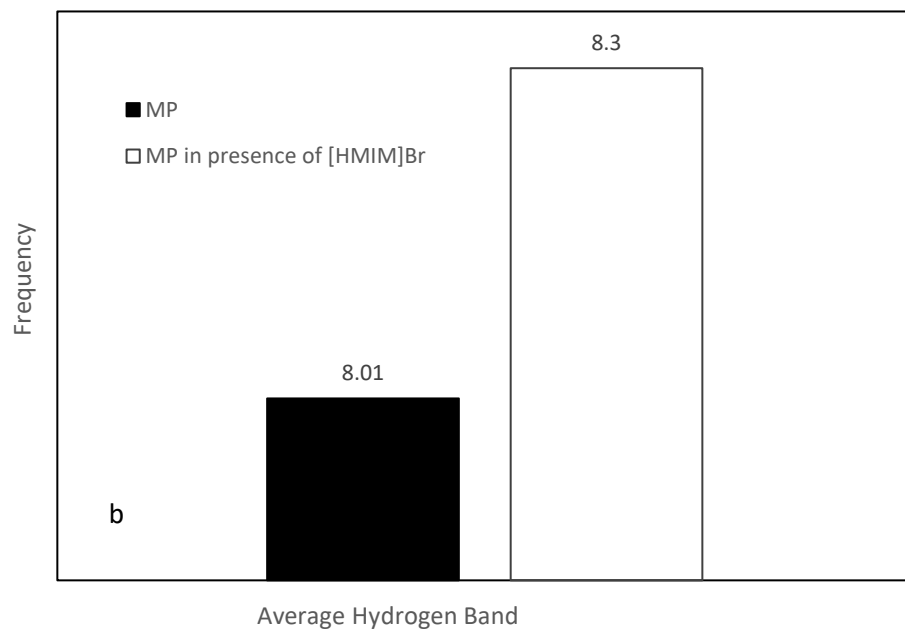
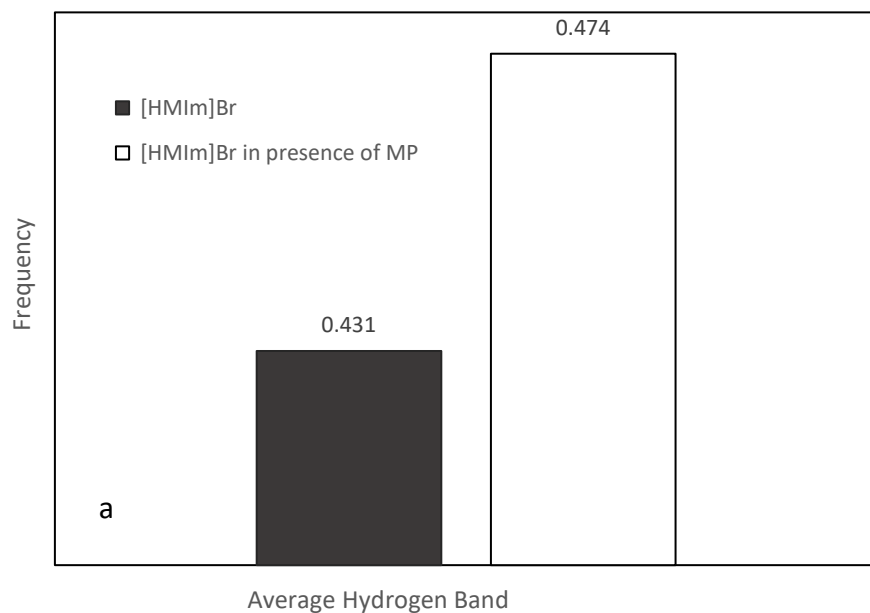


Fig. 10 The comparison of HB average values of [HMIm]Br in water and [HMIm]Br iMP+ water (a) MP in water and MP in [HMIm]Br + water (b)

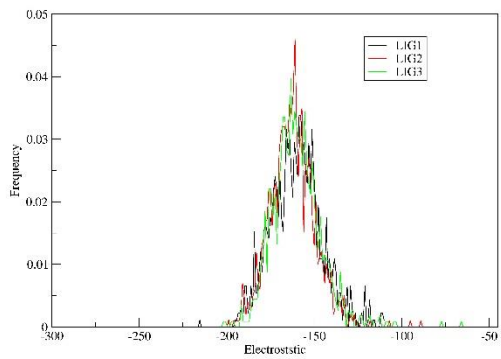
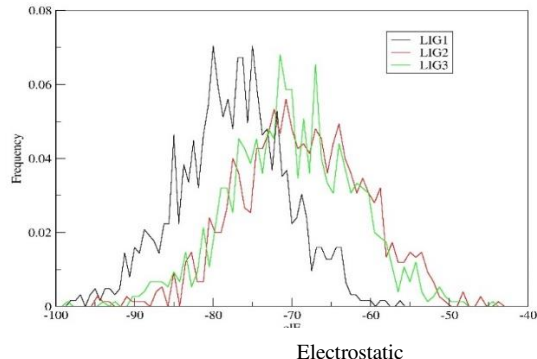
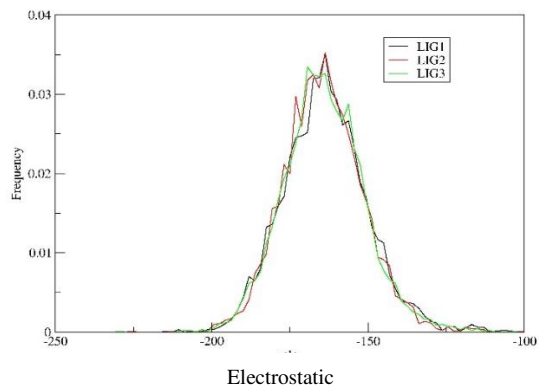
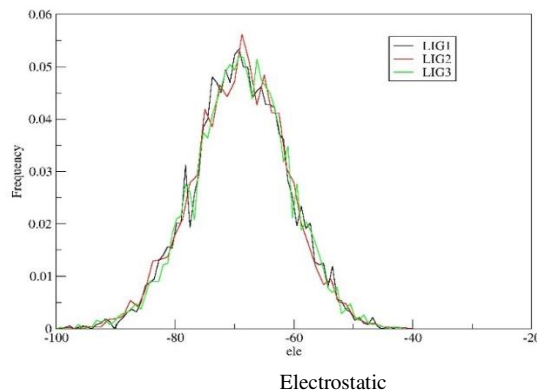
a**c****b****d**

Fig. 11. Normalized distribution of electrostatic of MP in water(a) [HMIm]Br in water, (a) HMIm]Br in MP + water (b), MP in water(c) and MP in HMIm]Br +water(d)

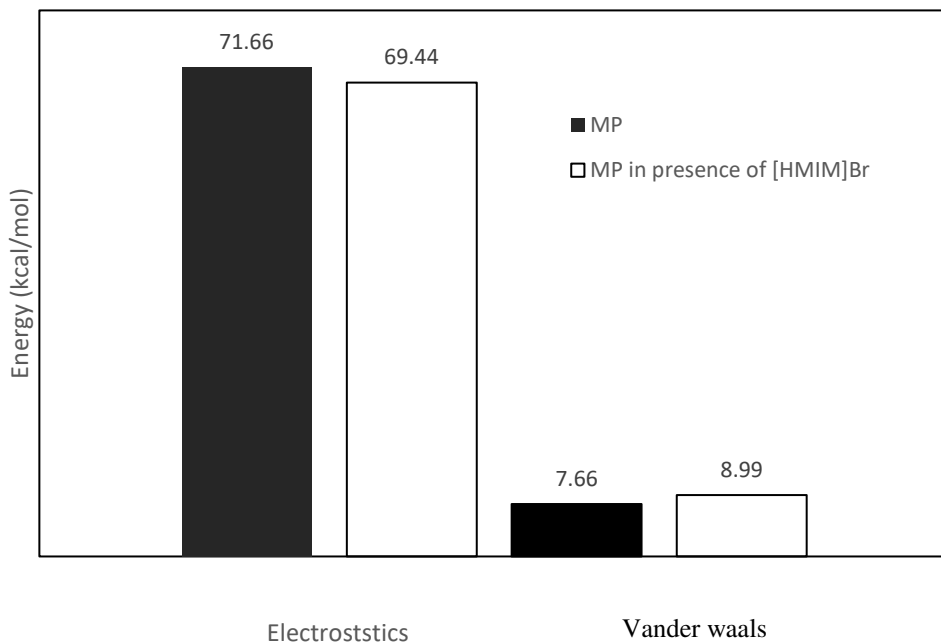


Fig. 12 The comparison of electrostatic and vander waals energies of MP in water and MP in [HMIm]Br + water

Table 1. Specification of the used component

Chemical Name	Source	Initial Massfraction Purity	Purification Method
N-methyl imidazole	Merck	>0.99	None
1-Bromohexane	Merck	>0.99	None
Ethyl acetate	Merck	>0.998	None
1 - hexyl - 3 - Methyimidazolium bromide	Senthesized	>0.99	Distillation
Methyl paraben (MP)	Sigma-Aldrich	>0.98	None

Table 2. Molar conductivities Λ_m of [HMIm]Br in different mixtures as a function of ILs molality (m_{IL}) on different

MP concentration (m_{MP}) at $T = (300.2 - 310.2 - 320.2)K$ and $P = 0.1$ MPa.

$m_{IL}(\text{mol} \cdot \text{kg}^{-1})$	$\Lambda^a(\text{S} \cdot \text{cm}^2 \cdot \text{mol}^{-1})$	$m_{IL}(\text{mol} \cdot \text{kg}^{-1})$	$\Lambda(\text{S} \cdot \text{cm}^2 \cdot \text{mol}^{-1})$	$m_{IL}(\text{mol} \cdot \text{kg}^{-1})$	$\Lambda(\text{S} \cdot \text{cm}^2 \cdot \text{mol}^{-1})$
$T = 300.2 \text{ K}$		$T = 310.2 \text{ K}$		$T = 320.2 \text{ K}$	
$m_{MP} =$					
0.000(mol.kg⁻¹)					
0.0012	131.43	0.0012	135.53	0.0012	137.63
0.0031	128.70	0.0031	131.63	0.0031	133.07
0.0051	127.47	0.0051	128.98	0.0051	130.89
0.0074	125.74	0.0074	126.75	0.0074	129.31
0.0097	124.57	0.0094	125.40	0.0094	128.71
0.0105	124.37	0.0105	124.28	0.0105	128.12
0.0396	110.55	0.0397	110.13	0.0397	114.48
0.0670	104.19	0.0670	104.53	0.0667	108.23
0.1097	97.84	0.1095	97.80	0.1093	101.36
0.1658	91.42	0.1654	91.99	0.1650	95.52
0.1968	88.80	0.1961	89.72	0.1958	92.94
$m_{MP} = 0.005$					
0.0012	129.17	0.0012	134.80	0.0012	135.25
0.0031	126.23	0.0031	127.92	0.0031	131.96
0.0054	125.20	0.0054	124.83	0.0054	130.39
0.0073	124.06	0.0073	122.43	0.0073	128.95
0.0096	122.29	0.0096	121.71	0.0096	128.22
0.0107	121.99	0.0108	121.45	0.0108	127.90
0.0401	107.97	0.0402	109.27	0.0398	112.93

0.0677	102.61	0.0674	104.05	0.0671	107.76
0.1108	96.69	0.1104	98.23	0.1098	100.97
0.1672	89.55	0.1669	92.27	0.1659	94.71
0.1983	86.70	0.1981	90.61	0.1971	92.13
$m_{MP} = 0.010$					
0.0011	126.86	0.0011	133.53	0.0011	133.60
0.0030	123.48	0.0030	125.06	0.0030	131.49
0.0052	122.45	0.0052	123.06	0.0052	130.15
0.0075	122.03	0.0075	122.43	0.0075	128.89
0.0097	121.24	0.0097	121.25	0.0097	127.52
0.0108	120.20	0.0108	120.70	0.0108	127.79
0.0399	108.13	0.0396	108.91	0.0396	112.77
0.0672	102.27	0.0670	103.25	0.0670	108.43
0.1101	89.16	0.1096	96.87	0.1094	103.79
0.1660	86.68	0.1656	90.81	0.1652	98.15
0.1970	85.25	0.1965	88.60	0.1961	95.99

^aThe average standard uncertainty of molar conductivity values were $u(\Lambda) = 0.18, 0.20$ and $0.21 \text{ S cm}^2 \text{ mol}^{-1}$ at $T = 300.2, 310.2$ and 320.2 K , respectively, $u(m) = 0.0001$ and $u(T) = 0.1 \text{ K}$

Table 3. Ion association constant (K_A), limiting molar conductivity (Λ_0) and thermodynamic functions ($\Delta G_A^\circ, \Delta H_A^\circ$ and ΔS_A°) at $T = (300.2, 310.2$ and $320.2) \text{ K}$ and $P = 0.1 \text{ MPa}$.

T/K	K_A ($\text{dm}^3 \cdot \text{mol}^{-1}$)	Λ_0 ($\text{S} \cdot \text{cm}^2 \cdot \text{mol}^{-1}$)	ΔG_A° ($\text{kJ} \cdot \text{mol}^{-1}$)	ΔS_A° ($\text{J} \cdot \text{mol}^{-1} \cdot \text{K}^{-1}$)	ΔH_A° ($\text{kJ} \cdot \text{mol}^{-1}$)	$R(\Lambda^\theta)$
$m_{MP} = 0.000 \text{ (mol.kg}^{-1})$						
300.2	12.43	136.42	-6.28	58.42	11.26	12.24

310.2	13.48	139.28	-6.70	60.34	12.02	11.30
320.2	16.81	142.83	-7.51	63.46	12.81	10.38
$m_{MP} = 0.005(\text{mol} \cdot \text{kg}^{-1})$						
300.2	12.59	134.13	-6.32	59.16	11.44	12.12
310.2	13.87	135.51	-6.78	61.25	12.22	11.15
320.2	17.09	142.02	-7.55	64.24	13.02	10.28
$m_{MP} = 0.010(\text{mol} \cdot \text{kg}^{-1})$						
300.2	13.24	132.32	-6.44	55.36	10.18	12.03
310.2	14.14	134.37	-6.82	57.05	10.87	11.11
320.2	17.37	138.93	-7.55	59.86	11.58	10.27

Table 4. Comparison of calculated molar conductivities (Λ_{NE}) with experimental data (Λ_m) at T=310.2K

$m_{MP}(\text{mol} \cdot \text{kg}^{-1})$	$\Lambda_{NE} (s \cdot \text{cm}^2 \cdot \text{mol}^{-1})$	$\Lambda_m (s \cdot \text{cm}^2 \cdot \text{mol}^{-1})$
$m_{[\text{HMIIm}]Br} (\text{mol} \cdot \text{kg}^{-1})$		

0.0105	0.000	122.4	124.28
	0.010		
0.0108		113.8	120.7

Table 5. Calculated average of RMSD for MP and [HMIIm]Br on different MP concentration ($m_{MP} = 0.000$ and $0.010 \text{ mol.kg}^{-1}$) at $T=310.2\text{K}$

RMSD [Å]			
$m_{MP} = 0.000 \text{ (mol.kg}^{-1})$	$m_{MP} = 0.010 \text{ (mol.kg}^{-1})$		
MP	[HMIIm]Br	MP	[HMIIm]Br
0.71	5.22	0.88	5.42

Table 6. Calculated average of H-Bondd for MP and [HMIm]Br on different MP concentration ($m_{MP} = 0.000$ and $0.010 \text{ mol.kg}^{-1}$) at $T=310.2\text{K}$

Number of H-bonds			
$m_{MP} = 0.000 \text{ (mol.kg}^{-1}\text{)}$		$m_{MP} = 0.010 \text{ (mol.kg}^{-1}\text{)}$	
MP	[HMIm]Br	MP	[HMIm]Br
8.01	0.431	8.30	0.474

Table 7. Calculated average of EL and vdw energies at $T=310.2\text{K}$

El		vdw	
[kcal.mol $^{-1}$]	[kcal.mol $^{-1}$]	[kcal.mol $^{-1}$]	[kcal.mol $^{-1}$]
$m_{MP} = 0.000 \text{ (mol.kg}^{-1}\text{)}$			
[HMIm]Br			
MP	MP	MP	[HMIm]Br
-71.66	-146.66	-7.66	-18.00
$m_{MP} = 0.010 \text{ (mol.kg}^{-1}\text{)}$			
-69.44	-164.83	-8.99	-18.82

Supplementary Files

This is a list of supplementary files associated with this preprint. Click to download.

- [Supportinginformation.docx](#)